# Electrofluorescence of MEH-PPV and Its Oligomers: Evidence for Field-Induced Fluorescence Quenching of Single Chains

**Timothy M. Smith, Nathaniel Hazelton, and Linda A. Peteanu***

*Department of Chemistry, Carnegie Mellon University, Pittsburgh, Pennsylvania 15213*

**Jurjen Wildeman***

*Department of Polymer Chemistry and Materials Science Centre, University of Groningen, Nijenborgh 4, 9747 AG Groningen, The Netherlands*

*Received: August 1, 2005; In Final Form: February 15, 2006*

Electrofluorescence (Stark) spectroscopy has been used to measure the trace of the change in polarizability ($tr\Delta\tilde{\alpha}$) and the absolute value of the change in dipole moment ($|\Delta\vec{\mu}|$) of the electroluminescent polymer poly[2-methoxy,5-(2′-ethyl-hexoxy)-1,4-phenylene vinylene] (MEH-PPV) and several model oligomers in solvent glass matrixes. From electrofluorescence, the measured values of $tr\Delta\tilde{\alpha}$ increase from 500 ± 60 Å$^3$ in OPPV-5 to 2000 ± 200 Å$^3$ in MEH-PPV. The good agreement found between these values and those measured by electroabsorption suggests the electronic properties do not differ strongly between absorption and emission, in contrast to earlier predictions. Evidence of electric-field-induced fluorescence quenching of MEH-PPV in dilute solvent glasses was found. When normalized to the square of the applied electric field, the magnitude of quench is comparable to that reported in the literature for thin films of MEH-PPV. In addition, fluorescence quenching was also observed in the oligomers with a magnitude that increases with increasing chain length. By using the values of $tr\Delta\tilde{\alpha}$ measured by electrofluorescence, a model is developed to qualitatively explain the chain length dependence to the fluorescence quench observed in the oligomers as a function of exciton delocalization along the oligomer backbone. Various explanations for the origin of this quenching behavior and its chain length dependence are considered.

## Introduction

Organic semiconducting polymers represent a novel class of materials being explored for application in photonic devices. They offer the ease of solution processing of polymers combined with the favorable optical and electronic properties of semiconductors for producing devices that equal or exceed their inorganic semiconducting counterparts.[1,2] Optoelectronic devices constructed from these materials have been the focus of intense industrial and academic research for nearly two decades. Applications ranging from transistors,[3−6] organic light-emitting diodes (OLEDs),[1,2,7] and photovoltaic cells,[8−10] to large-area flat panel displays[11] are already being integrated into public and industrial use with more exotic applications, such as polymer-based lasers,[12−14] rapidly approaching commercialization. Important examples within this novel class of materials include poly(*p*-phenylenevinylene) (PPV) and its derivatives such as poly[2-methoxy-5-(2-ethylhexyloxy)-*p*-phenylenevinylene] (MEH-PPV) (Scheme 1). Understanding the optical and electronic properties of their lowest-energy electronic states, which are the intermediaries in electroluminescent and photovoltaic processes,[15] is critical to optimizing performance in photonic applications. Stark absorption spectroscopy or electroabsorption (EA) has been previously used to ascertain how chain length, chain conformation, and the properties of the matrix containing PPV and related derivatives affect the electronic properties of the lowest-energy excitation, the singlet exciton ($S_1$).[16−21]

**SCHEME 1: Molecular Structures of (a) MEH-PPV and (b) OPPV-*n*, Where *n* = 3, 5, 9, and 13 and R = $OC_8H_{17}$**

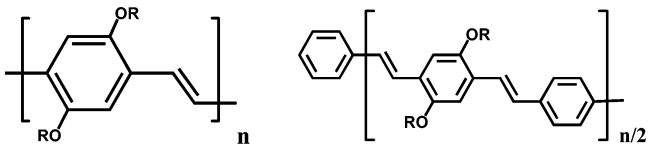


While the results from EA have demonstrated how aggregation and molecular disorder affect the optical and electronic properties of $S_1$ in the Franck−Condon (FC) region, both photoluminescence and electroluminescence originate from the *relaxed* singlet ($S_1$) excited state.[1,2,15,22,23] Questions related to the relaxed $S_1$ state include how its electronic properties influence charge injection and charge transport efficiencies in semiconducting polymers, as well as the maximum achievable quantum efficiency in electroluminescent and photovoltaic devices. The properties of this state may be probed by electrofluorescence (EF).[24,25]

EA and EF permit the measurement of two fundamental electronic properties of a molecule, namely, the trace of the change in polarizability $tr\Delta\tilde{\alpha}$ and the absolute value of the change in dipole moment $|\Delta\vec{\mu}|$ between the initial and final states in the absorption and emission processes, respectively. This is done by analysis of the shift in the absorption (EA) or emission (EF) band of a frozen isotropic sample in an applied electric field. Frequently associated with the size of the exciton, $tr\Delta\tilde{\alpha}$ is also related to charge mobility through the molecular

* Corresponding authors. E-mail: peteanu@andrew.cmu.edu (L.A.P.); j.wildeman@rug.nl (J.W.).

10.1021/jp054264p CCC: $30.25 
Published on Web 03/30/2006

backbone.[16,26−28] Electronic transitions in a molecule also cause redistribution of charge and the extent of charge transfer that occurs can be ascertained from $|\Delta\vec{\mu}|$. This quantity is relevant to the operation of photovoltaic devices in which mobile charge carriers are generated within the polymer layer by light absorption. Photogeneration of charge carriers occurs when exciton dissociation occurs either through electron-transfer reactions[8,29−32] or by an external electric field.[33−44] A large $|\Delta\vec{\mu}|$ would be expected for charge-transfer reactions in the polymer layer that do not result in complete exciton dissociation. As charge-transfer reactions can lead to a large observed $|\Delta\vec{\mu}|$, so too can molecular conformation disorder. Though, in symmetric molecules, $|\Delta\vec{\mu}|$ is expected to be zero, molecular conformational disorder can break the symmetry of the molecule, thereby allowing a substantial $|\Delta\vec{\mu}|$ to be observed.[17,21]

The electronic properties of the FC and relaxed excited state are presumably identical if a symmetric relationship exists between light absorption and emission. This is typically the case for unreactive systems and those that do not undergo substantial geometric or electronic changes as they evolve on the excited-state surface. Contrary to this prediction, Hogiu et al. found a discrepancy between the $tr\Delta\vec{\alpha}$ values measured in the FC region by using EA on MEH-PPV and its oligomers in frozen glasses and those that had been obtained previously from time-resolved microwave conductivity (TRMC) measurements in dilute solution.[21,26−28] An important distinction between the two methods is that TRMC reports on the electronic properties of the relaxed $S_1$ state and is therefore sensitive to the effects on the molecular polarizability of changes in nuclear geometry that occur after photoexcitation. The current contribution reports on the results of EF measurements that are aimed at understanding the disparity between the EA and TRMC results.

There are a number of examples in the literature for which the electronic properties of the final state are significantly different from those of the FC state. These include diphenylpolyenes[45,46] that photoisomerize, dyes at colloidal−semiconductor interfaces that undergo charge injection,[47] and the photosynthetic reaction center.[48,49] In the case of conjugated polymers, one effect that could potentially cause an increase in polarizability between the FC region and the excited-state minimum (and therefore an increase in $tr\Delta\vec{\alpha}$) is the increase in planarization of the molecular backbone that is known to occur prior to emission.[15,50,51] This would be expected if planarization leads to weaker electron−electron correlation in the relaxed excited-state, meaning exciton delocalization extends further along the molecular backbone.[26,51−54] Comparison of excited-state polarizabilities measured via EA and EF would then reveal whether the electronic delocalization indeed increases in the relaxed excited state prior to photoluminescence. Interestingly, the results presented here show little evidence that the electronic properties differ greatly between absorption and emission, in contrast to earlier predictions.

One significant difference that we observe between the EF and EA results for the molecules studied here is that the applied field measurably decreases the fluorescence intensity while its effect on the absorption intensity is minimal. Electric-field-modulated fluorescence (EMF) of PPV-like polymers has been previously reported in the literature.[33−40,42−44] The effect was modeled as arising from field-induced exciton dissociation to create a nonradiative state either directly via the formation of free charges or indirectly via the formation of a charge-transfer state. Expanding on this work, EMF studies by Pfeffer et al. identified a correlation between polarizability in the relaxed $S_1$ state and the magnitude of luminescence quenching by studying electric-field effects on poly(*p*-phenylene phenylenevinylene) (PPPV) thin film photoluminescence.[42] Early studies of the magnitude of the field-induced quench showed that it is greater in polymers with extended structures, such as PPPV,[37,41,42] than in a molecular species (tris(stilbene)amine or TSA).[38] In this paper, we report in detail on the correlation between magnitude of field-induced fluorescence quenching and effective conjugation length by systematically varying the conjugation length from short oligomers to the polymer, MEH-PPV.

Likewise, earlier studies that examined the concentration effect on the magnitude of the field-induced quench for PPPV in a polycarbonate host found that, while the effect becomes much more pronounced at higher concentrations, presumably due to intermolecular interactions or charge transfer between chains, it is nonzero at lower concentrations. These measurements led Vissenberg and de Jong to propose a mechanism for *on-chain* field-induced exciton dissociation.[55] This interpretation was challenged by Conwell, who pointed out that phase segregation of PPPV within the polycarbonate host matrix would lead to regions of high dopant concentration where intermolecular exciton dissociation would dominate.[56] Here, we report field-induced quenching on samples that are over a factor of 100 more dilute than those used by Deussen et al. in ref 38. Moreover, these samples are isolated in organic solvent glasses rather than polycarbonate films to further diminish the likelihood of having locally concentrated regions. *By eliminating interchain interactions through the use of dilute samples of model oligomers, we affirm that fluorescence quenching can indeed be observed on isolated chains, though it becomes somewhat more pronounced in systems such as in MEH-PPV where interchain interactions can exist.*

## Experimental Methods

**Sample Preparation.** MEH-PPV (av MW: $1 \times 10^5$) and the oligophenylenevinylenes (OPPVs) were synthesized by Dr. Jurjen Wildeman.[57,58] The polymer and oligomers were dissolved in 2-methyltetrahydrofuran (2-MTHF) and allowed to stir for approximately 1 to 2 weeks prior to use in an experiment. Two indium−tin oxide (ITO) coated glass slides were used to construct an optical cell incorporating a $110 \pm 4$ $\mu$m or a $65 \pm 3$ $\mu$m Kapton spacer; the latter being used to apply higher fields to the sample. The optical density (OD) of the polymer samples was found to be 0.01−0.04 (monomer unit concentration $10^{-4}$ to $4 \times 10^{-3}$ M) and that of the oligomers was 0.01−0.2 (monomer unit concentration $10^{-4}$ to $3 \times 10^{-5}$ M). Solutions used for EF were consistently 10−100-fold more dilute than this to minimize self-absorption effects. Although similar results were obtained from the analysis of EF spectra from samples at concentrations down to $6 \times 10^{-8}$ M, the signal-to-noise of these data was somewhat poorer than that reported here. Optical quality glasses were formed by rapid immersion of the samples into an optical Dewar (H. S. Martin) filled with liquid nitrogen. Transmission polarization measurements confirmed that the samples are isotropic as low-temperature solvent glasses (data not shown).

**Instrumentation.** The electroabsorption apparatus is home-built and has been described in detail previously.[21] Briefly, a 0.3 m single monochromator (Spex) with 3−5 nm spectral resolution disperses light from a 150 W xenon arc lamp or 250 W quartz tungsten lamp (both from Oriel). After exiting the monochromator, the spectrally narrow excitation light is horizontally polarized by using a Glan−Thomson polarizer. In this way, the angle between the direction of polarization of the electric field of the incident light and direction of the electric

field vector of the applied AC voltage is defined. An AC electric field on the order of $10^6$ V/cm was applied across the sample by using a high-voltage power supply (Joseph Rolfe) that was modulated at 470 Hz for EA spectra and 55 Hz for EF spectra. For EA measurements, the light transmitted through the sample is detected by a photodiode (UDT-020UV). The small changes in the amount of transmitted light (EA spectra) or in the fluorescence emission (EF spectra) produced by the applied electric field are measured by using phase-sensitive lock-in detection at the second harmonic of the AC field frequency.

EF measurements are conducted on a Fluorolog-2 instrument (Spex) with 1 nm resolution and a room-temperature photomultiplier detector (Hamamatsu R928P). The same optical Dewar containing the sample in EA measurements is employed, but the cell is oriented for front-face excitation geometry. To minimize any contribution to the EF spectrum due to AC−Stark effects on the extinction coefficient at the excitation wavelength, each sample was excited at the zero crossing of its respective EA spectrum. Calibration of the fluorometer with a mercury pen-lamp and fluorescein standard prepared in 1 M NaOH (Fisher Scientific) was conducted prior to EF measurements to ensure spectral accuracy. A signal-to-noise ratio consistently exceeding ~5 was achieved in EF for samples having fluorescence intensities on the order $2 \times 10^6$ counts per s. Because the emission spectrum is obtained simultaneously with the EF spectrum, no spectral correction of the absolute fluorescence was performed.

**Data Fitting.** The analysis of EA data follows that in the literature.[21,24,59] Because the samples are embedded isotropically in a rigid glass, the following equations presented are appropriate. The change in absorption due to the application of an external electric field is fit to the weighted sum of zeroth, first, and second derivatives of the zero-field absorption spectrum. The overall change in absorbance caused by the application of an electric field can be described by eq 1,

$$\Delta A(\tilde{\nu}) = \vec{\mathbf{F}}_{\text{eff}}{}^2\left[\mathbf{a}_\chi A(\tilde{\nu}) + \mathbf{b}_\chi \frac{\tilde{\nu}}{15\hbar}\left\{\frac{\partial}{\partial\tilde{\nu}}\left(\frac{\mathrm{A}(\tilde{\nu})}{\tilde{\nu}}\right)\right\} + \mathbf{c}_\chi \frac{\tilde{\nu}}{30\hbar^2}\left\{\frac{\partial^2}{\partial\tilde{\nu}^2}\left(\frac{A(\tilde{\nu})}{\tilde{\nu}}\right)\right\}\right] \quad (1)$$

The term $\boldsymbol{A}(\tilde{\nu})$ represents the unperturbed absorption as a function of wavenumber ($A(\tilde{\nu})$), and $\vec{\boldsymbol{F}}_{\text{eff}}$ represents the field at the sample in V/cm. This effective field includes the enhancement of the applied field due to the cavity field of the matrix. The subscript $\chi$ represents the angle between the direction of the applied electric field and the electric field vector of the linearly polarized light. The experiments reported here were performed at $\chi = 54.7°$ (magic angle). The magic angle is determined from the relevant refractive indices of the light propagation medium (i.e., liquid nitrogen and 2-MTHF). At $\chi = 54.7°$, the expressions of $\mathbf{a}_\chi$, $\mathbf{b}_\chi$, and $\mathbf{c}_\chi$ are related to the change in the transition moment polarizability ($\boldsymbol{A}_{ij}$) and hyperpolarizability ($\boldsymbol{B}_{ij}$), the average change in electronic polarizability $\langle\Delta\vec{\alpha}\rangle$, and the change in dipole moments $|\Delta\vec{\mu}|$, respectively, as given in eqs 2−4.[21]

$$a_{54.7} = \frac{1}{3|\vec{m}|^2}\sum_{i,j}\mathbf{A}^2 + \frac{2}{3|\vec{m}|^2}\sum_{i,j}\vec{m}_i\mathbf{B} \quad (2)$$

$$b_{54.7} = \frac{10}{|\vec{m}|^2}\sum_{i,j}\vec{m}_i\mathbf{A}\Delta\vec{\mu}_j + \frac{15}{2}\langle\Delta\vec{\alpha}\rangle \quad (3)$$

$$c_{54.7} = 5|\Delta\vec{\mu}|^2 \quad (4)$$

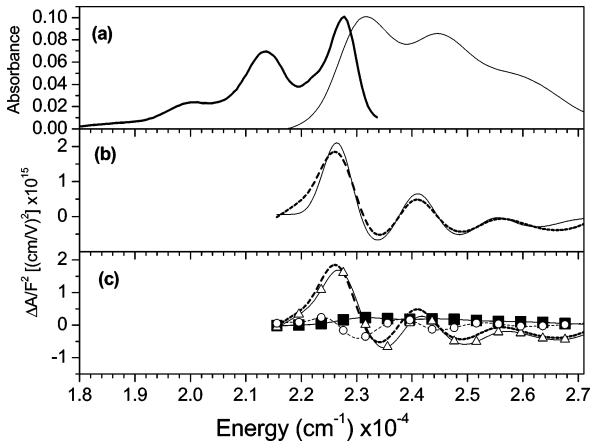


**Figure 1.** Stark absorption and emission spectra of OPPV-3 in 2-MTHF glass. Fluorescence spectra shown in panel a. Panel b contains the EA spectrum (solid line) and the fit (dashed line). Panel c shows the zeroth (-■-), first (-△-), and second (-○-) derivative components of the fit (bold dashed line) to the EA spectra. The low SNR in fluorescence-prohibited acquisition of electrofluorescence spectrum. See Discussion.

In these equations, **A** and ***B*** denote the transition polarizability and hyperpolarizability, respectively and describe the effect of $\boldsymbol{F}_{\text{eff}}$ on the molecular transition moment ($\vec{m}$): $\vec{m}\,(\vec{F}_{\text{eff}}) = \vec{m} + \mathbf{A}\cdot\vec{F}_{\text{eff}} + \vec{F}_{\text{eff}}\cdot\boldsymbol{B}\cdot\vec{F}_{\text{eff}}$. These terms are generally small for allowed transitions and can therefore be neglected relative to other terms in the expression for $\langle\Delta\vec{\alpha}\rangle$ (eq 3). Here we quote ($tr\Delta\vec{\alpha}$), the trace of the change in polarizability between the ground and excited states [i.e., $\langle\underline{\Delta\alpha}\rangle = {}^1/_3(tr\Delta\vec{\alpha})$]. Information regarding $|\Delta\vec{\mu}|$ is contained in the $\boldsymbol{c}_{54.7}$ term. As the samples studied in this report are randomly oriented in solvent glasses, only the magnitude of $\Delta\vec{\mu}$ and not its sign is measured. If the fit to the EA or EF data is of high quality when using a single set of $\boldsymbol{a}_{54.7}$, $\boldsymbol{b}_{54.7}$, and $\boldsymbol{c}_{54.7}$ parameters, this indicates that the electronic properties of molecules remain consistent across the entire absorption or emission band, respectively. Analysis of the EF data using eqs 2−4 is the same as that for EA spectra, with the exception that the fluorescence spectra are normalized to energy (wavenumber) cubed.

## Results and Discussion

To understand the photoluminescent and electroluminescent properties of conjugated polymers, it is critical to understand the electronic properties of the first excited state to which absorption is one-photon allowed. For molecules of approximate $C_{2h}$ symmetry, such as those studied here, this state is designated by the symmetry label $1B_u$. Here we compare the electronic properties of the FC and relaxed excited states of MEH-PPV and several related oligomers by using EA and EF spectroscopy, respectively. The top panels of Figures 1−5 show the absorption and fluorescence spectra of each oligomer and the polymer. The fluorescence spectra of the oligomers red-shift with increasing conjugation length and exhibit structure due to the C═C stretching vibrations (~1500 cm$^{-1}$). Whereas the vibronic structure is less well resolved in the oligomer absorption spectra, it is quite apparent in the associated EA signals.

The middle and bottom panels of Figures 1−5 show the EA (left-hand panel) and EF (right-hand panel) spectra of OPPVs of 3, 5, 9, and 13 rings in length as well as the polymer MEH-PPV. EF data for OPPV-3 are not included, as its EF response is below our present detection limit. Judging by their high correlation coefficients ($R^2$ between ~0.988 and 1), the fits to all of the EA and EF spectra are of high quality, indicating that

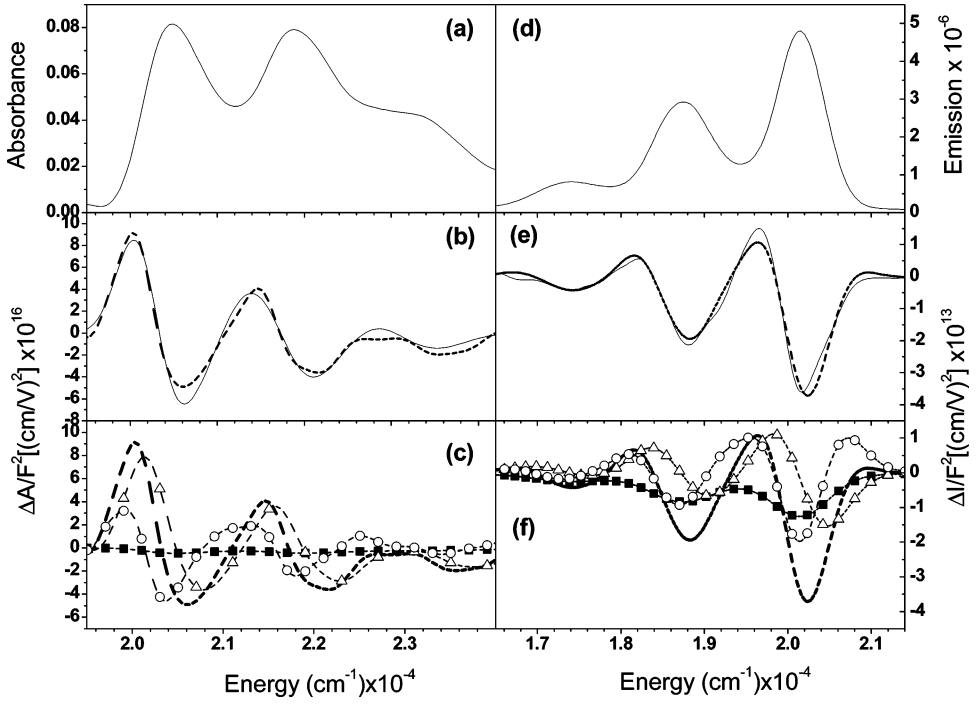


**Figure 2.** Stark absorption and emission spectra of OPPV-5 in 2-MTHF glass. Low temperature absorption (panel a) and fluorescence (panel d) are shown. The EA and EF spectra (solid lines) and their corresponding fits (dashed lines) are contained in panels b and e, respectively. Panels c and f show the zeroth (-■-), first (-△-), and second (-○-) derivative components of the fit (bold dashed line) to the EA and EF spectra.

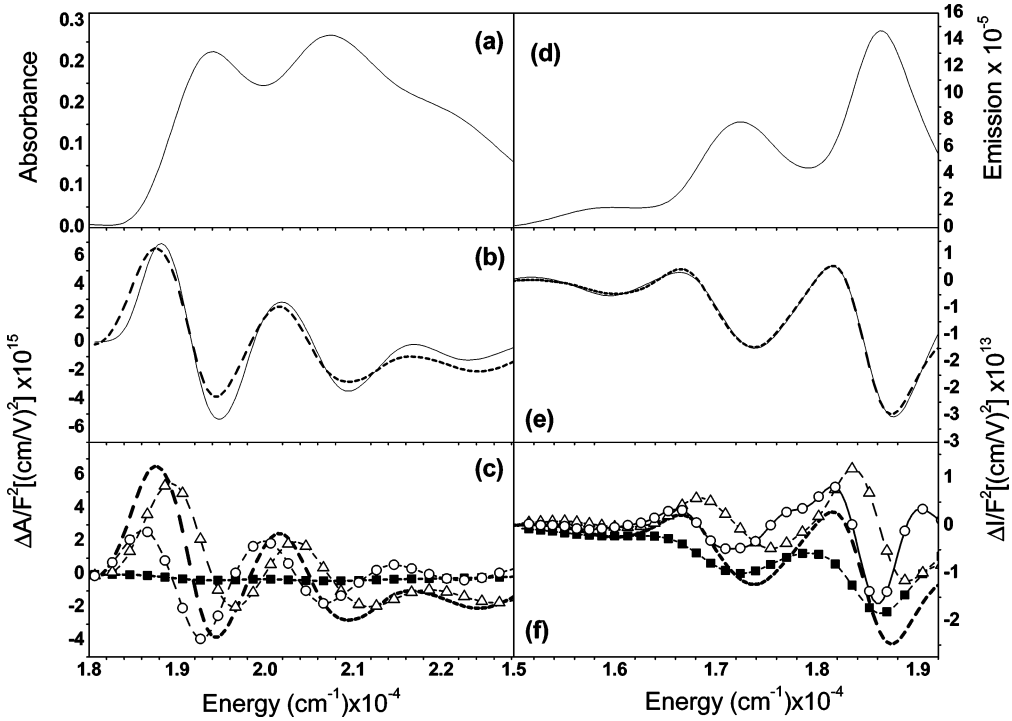


**Figure 3.** Stark absorption and emission spectra of OPPV-9 in 2-MTHF glass. Low temperature absorption (panel a) and fluorescence (panel d) are shown. The EA and EF spectra (solid lines) and their corresponding fits (dashed lines) are contained in panels b and e, respectively. Panels c and f show the zeroth (-■-), first (-△-), and second (-○-) derivative components of the fit (bold dashed line) to the EA and EF spectra.

the electronic properties of these molecules are uniform across the absorption and emission bands. The electronic properties $|\Delta\vec{\mu}|$ and $tr\Delta\tilde{\alpha}$ for the transition between the ground ($A_g$) and both the Franck−Condon (EA) and relaxed (EF) $1B_u$ excited states derived from these fits are summarized in Table 1. The EA data for MEH-PPV and OPPV-9 have been previously reported by our group and are included for comparison.[21]

An examination of the Stark spectra and associated table of molecular parameters reveals three dominant trends: (1) both $|\Delta\vec{\mu}|$ and $tr\Delta\tilde{\alpha}$ increase with oligomer conjugation length (Figures 6 and 7), (2) for each molecule, the $tr\Delta\tilde{\alpha}$ measured in EF is similar to or smaller than that measured by EA, and (3) electric-field-induced fluorescence quenching is observed as a nonzero amplitude of the zeroth-derivative component ($\alpha_{54.7}$ in eq 2) of the EF line-shape that is *not* seen in the corresponding EA spectrum. These observations are discussed in turn below.

The degree of charge transfer in the relaxed excited state of these oligomers is given by the value of $|\Delta\vec{\mu}|$ measured in EF.

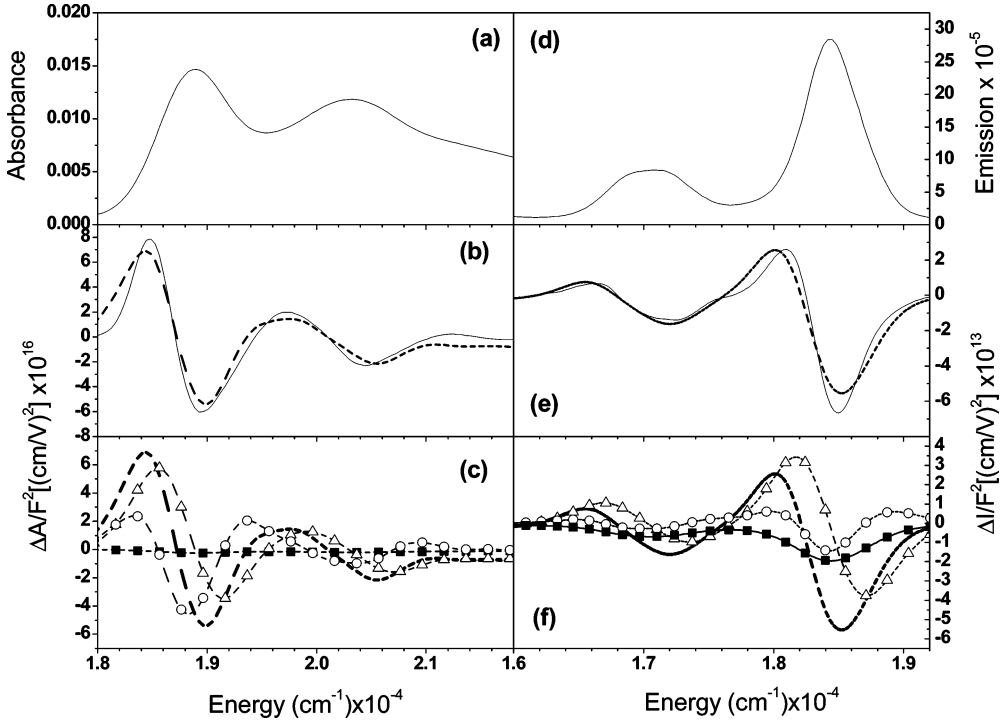


**Figure 4.** Stark absorption and emission spectra of OPPV-13 in 2-MTHF glass. Low temperature absorption (panel a) and fluorescence (panel d) are shown. The EA and EF spectra (solid lines) and their corresponding fits (dashed lines) are contained in panels b and e, respectively. Panels c and f show the zeroth (-■-), first (-△-), and second (-○-) derivative components of the fit (bold dashed line) to the EA and EF spectra.

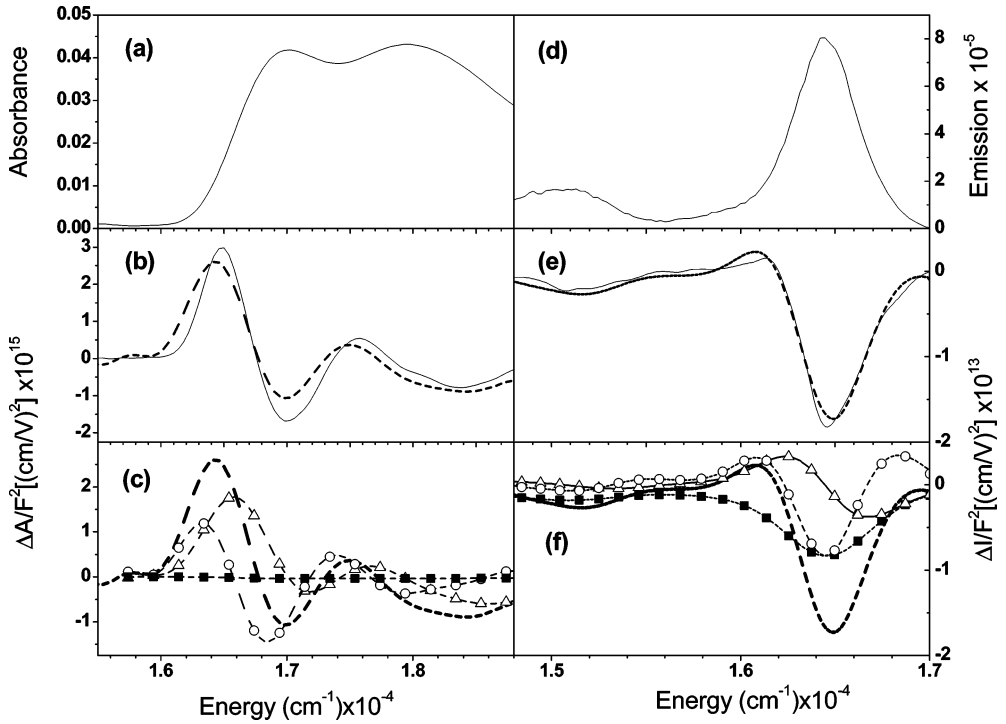


**Figure 5.** Stark absorption and emission spectra of MEH-PPV in 2-MTHF glass. Low temperature absorption (panel a) and fluorescence (panel d) are shown. The EA and EF spectra (solid lines) and their corresponding fits (dashed lines) are contained in panels b and e, respectively. Panels c and f show the zeroth (-■-), first (-△-), and second (-○-) derivative components of the fit (bold dashed line) to the EA and EF spectra.

Because all of the oligomers studied here are nominally of $C_{2h}$ symmetry, they are not expected to possess a dipole moment in either the ground or excited electronic state. Nonetheless, a significant $|\Delta\vec{\mu}|$ associated with both absorption and emission is observed (Table 1 and ref 21). The magnitude of $|\Delta\vec{\mu}|$ increases with increasing conjugation length (~3−10 D), as was previously seen in EA (see Figure 6).[21] The nonzero $|\Delta\vec{\mu}|$ of PPV derivatives in glassy solvents was modeled in ref 21 as arising from a combination of two effects: (1) solvent-induced conformational disorder of the molecule (inner-sphere disorder) and (2) local asymmetric electrostatic fields generated by the random orientation of solvent molecules that induce dipole

**TABLE 1: Parameters Obtained from Electroabsorption, and Electrofluorescence**

| | electroabsorption | | electrofluorescence | | fluorescence quench (%) | |
|---|---|---|---|---|---|---|
| oligomer | $(\|\Delta\mu\|)^b$ | $tr\langle\Delta\alpha\rangle^a$ | $(\|\Delta\mu\|)^b$ | $tr\langle\Delta\alpha\rangle^a$ | $a_\chi$-quench[d] | AC-EMF |
| OPPV-3 | $2.0 \pm 0.8$ | $140 \pm 40$ | | | | |
| OPPV-5 | $4.0 \pm 0.1$ | $500 \pm 90$ | $5.0 \pm 0.1$ | $500 \pm 60$ | $0.034 \pm 0.001$ | $0.030 \pm 0.008$ |
| OPPV-9 | $9.0 \pm 0.2$ | $2000 \pm 200$ | $7.0 \pm 0.5$ | $1900 \pm 530$ | $0.12 \pm 0.01$ | $0.11 \pm 0.01$ |
| OPPV-9[c] | $7 \pm 1$ | $2000 \pm 200$ | | | | |
| OPPV-13 | $9.0 \pm 0.1$ | $2000 \pm 200$ | $9 \pm 2$ | $2900 \pm 850$ | $0.27 \pm 0.04$ | $0.26 \pm 0.02$ |
| MEH-PPV | $10 \pm 1$ | $3000 \pm 600$ | $14 \pm 3$ | $2000 \pm 210$ | $0.55 \pm 0.01$ | $0.50 \pm 0.03$ |
| MEH-PPV[c] | $11 \pm 1$ | $2000 \pm 200$ | | | | |

[a] In Å$^3$. [b] In Debye (D). Average and standard deviation in $(|\Delta\mu|)$ and $tr\Delta\alpha$ are calculated by fitting individual replicates of EA and EF spectra (see text) and averaging the results obtained from different field strengths. [c] From ref 21. [d] Quenching efficiencies calculated from the zeroth derivative as described in the text.

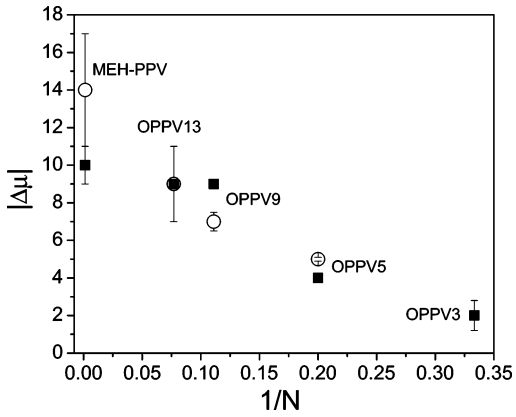


**Figure 6.** The value of $|\Delta\mu|$ of the $1B_u$ state measured in electroabsorption (-○-) and in electrofluorescence (-■-) vs $1/N$, where $N$ is the chain length measured in phenyl rings.

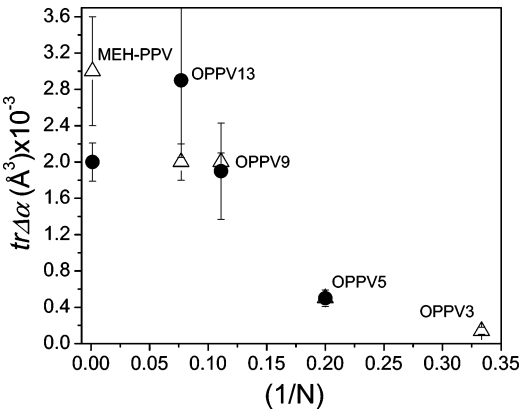


**Figure 7.** The value of $\boldsymbol{tr}\Delta\alpha$ of the $1B_u$ state measured in electroabsorption (-△-) and in electrofluorescence (-●-) vs $1/N$, where $N$ is the chain length measured in phenyl rings.

moments in the molecule through its $tr\Delta$ (outer-sphere disorder). Similar effects appear to be operative in EF spectra of these systems.

The values of $tr\Delta\tilde{\alpha}$ obtained from EF places the observed oligomer and polymer polarizabilities on the lower end of the 400−20 000 Å$^3$ range obtained previously for MEH-PPV and PPV using EA.[18,20,21,60−62] Supporting the results reported here and in ref 21 is the fact that our values of $tr\Delta\tilde{\alpha}$ are in quantitative agreement with those calculated using INDO/SCI coupled with finite-field methods.[21] A comparison of $tr\Delta\tilde{\alpha}$ between the longest oligomers (OPPV-9 and OPPV-13) and MEH-PPV suggests the saturation length for this property is ∼13 PV units. This value is slightly larger than the estimate of ∼10 PV units for the conjugation length of MEH-PPV based on the inverse chain-length dependence of the excitation energy in the oligomers.[63] Similar trends in $tr\Delta$ with conjugation length were identified in TRMC measurements though the published TRMC values for $tr\Delta$ of MEH-PPV and 3-, 5-, and 9-mers are ∼2−4 times larger than those reported here.[26−28] One possible explanation for this difference is that, although both methods probe the relaxed excited state, the TRMC sample is in solution permitting greater planarization of the molecule prior to emission. This, in turn, should give rise to a larger $tr\Delta\tilde{\alpha}$ due to increased conjugation in the chain. In contrast, EF data is obtained in rigid matrixes such as solvent glasses or polymer films where molecular mobility is strongly reduced. Consistent with the expectation that the geometries of molecules in glasses are similar in their Franck−Condon and emissive states is the observation that the values of $tr\Delta\tilde{\alpha}$ obtained in EA and in EF are similar as well.

A somewhat surprising result is the similarity between the parameters measured in EA and EF for MEH-PPV given that the emitting state is likely to be more characteristic of longer chain segments than the absorbing state due to rapid energy migration along the chain.[64−68] One reason that our experiment appears to be insensitive to the effects of energy migration may be that the saturation length for $tr\Delta\tilde{\alpha}$ of only ∼13 PV units, meaning that transfer to longer segments would not cause the polarizabilities measured in emission to be larger than those measured in absorption, at least to within the precision of our results.

Focusing on the zeroth-derivative component of the EF spectra (solid line in the bottom-right panels of Figures 2−5), its contribution relative to those of the other two components is at least 3 orders of magnitude greater for each molecule than in its corresponding EA spectrum. The presence of a negative zeroth-derivative component in the EF spectra indicates that the applied field quenches the emission intensity. Normally, a substantial zeroth-derivative component in the EA spectrum is attributed to a change in the oscillator strength of the absorption transition such as might be due to a field-induced mixing with other nearby states.[18,60,62,69−71] Were this to be the case, the emission intensity would consequently be affected. However, the fact that the zeroth-derivative component in the EA spectrum is negligible rules out the possibility of a field-induced change in oscillator strength as a source of the observed decrease in fluorescence intensity with applied field. This conclusion is in agreement with previous results in which an applied field altered the fluorescence lifetime of MEH-PPV but not its early time (<1 ps) transient photoluminescence signal.[40]

By examining the line shape of the emission quenching, we see that it follows that of the emission spectrum itself. In other words, there appears to be no emission energy dependence to the degree of quench in any of the molecules studied. Therefore, there is no indication that the quenching occurs primarily within a subset of the species that might be present in the glass, such as aggregates. If quenching were favored in aggregated species,

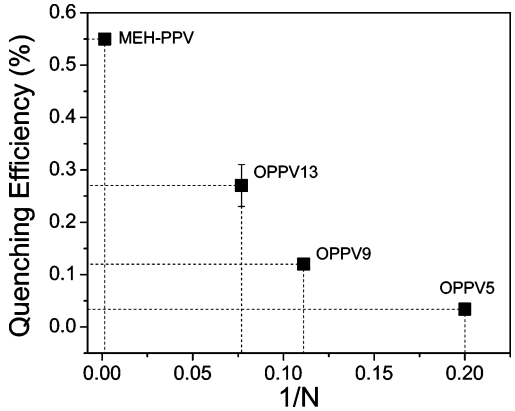


**Figure 8.** Inverse chain length dependence of quenching efficiency. Vertical bars indicate standard deviations. *N* is the number of contiguous double bonds along the shortest path between oligomer end carbons. Quenching data (-■-) calculated from electrofluorescence spectra measured using applied field strength of ~0.3MV/cm.

we might see the quenching efficiency be greater at the red edge of the emission spectrum where aggregates predominately emit. Furthermore, fluorescence depolarization studies have shown no evidence of aggregation in oligomer solvent glasses.[72] As an aside, our observation that the quenching is independent of emission energy is inconsistent with the results of Pfeffer et al., who observed marked increase in the extent of quenching on the blue edge of the fluorescence emission spectra in poly-[*p*-terphenylene vinylene)] (PPTV).[33,38,42]

In Figure 8 is contained a plot versus inverse chain length ($1/N$) of the field-induced quenching efficiency ($\delta_{fl}(\vec{F})$). The latter is defined as the magnitude of the zeroth-derivative component ($\alpha_{54.7}$ in eq 2), which is the change of the fluorescence intensity in the presence and absence of the applied field, divided by the zero-field emission spectrum ($I_0$) expressed as a percent (eq 5).

$$\delta_{fl}(\vec{F}) = \frac{\alpha_{54.7}}{I_o} \times 100\% \qquad (5)$$

This graph shows that quenching efficiency increases with increasing oligomer chain length and approaches ~0.6% in the polymer limit for an applied field of 0.3MV/cm.

Deriving quenching efficiencies from the zeroth derivative component of the Stark spectrum is unconventional, considering that all accounts of field-induced quench reported in the literature were obtained from electric-field-modulated fluorescence (EMF). In EMF, an electric field is applied to the sample and its effect on the integrated fluorescence spectrum is measured. Though DC fields are typically used in EMF, AC fields have been utilized as well. The effect of the AC field on the fluorescence intensity is comparable to DC fields because the intensity changes in response to the root-mean-squared amplitude of the AC field, regardless of the field polarity. By measuring the quench induced by an AC field, we can corroborate the quenching efficiencies derived from the zeroth derivative of the EF spectra. To explore the effect of an AC field on the integrated fluorescence spectrum, much of the original EF setup was retained, with the difference being that the grating was replaced by a mirror, allowing measurement of the integrated fluorescence intensity. We find the results from AC-EMF are in excellent agreement with those derived from the zeroth derivative method (Table 1). *Therefore, the zeroth derivative of the EF spectrum is a reliable measure of field-induced quenching.*

To gain some insight into the mechanism for this process, we next compare the magnitude of the field-induced quenching seen here to that reported for MEH-PPV and related polymers in the literature.[33−37,39−44] To facilitate comparison among experiments that have been performed at different applied field strengths, we use the result of ref 35 that the percent quenching is expected to vary in proportion to the square of the applied field strength. After scaling the various quenching efficiencies reported for MEH-PPV to an applied field of 0.3 MV/cm, we see that the magnitude of the field-induced luminescence quench observed here for MEH-PPV (~0.6% at 0.3 MV/cm) falls within a fairly broad range of values (0.3−1.1%) that have been reported in the literature.[37,39−41,44,73] It is important to emphasize that the magnitude of the quench and the mechanism that brings it about depend critically on the specifics of the sample preparation and electrode configuration that is used. This is discussed below.

One important experimental parameter is whether the sample configuration minimizes charge injection into the sample as free charges are known to effectively quench luminescence of PPV-like molecules.[74−79] One means of doing this is to coat the electrodes with a blocking layer.[39,44] Alternatively, if the sample cell is an electroluminescent device consisting of one electrode that is a hole injector, such as ITO, and the other an electron injector, such as aluminum, the device is run in reverse bias.[42] In the experiments reported here, charge injection is minimized by the use of two identical ITO electrodes and by applying an AC rather than DC voltage to the cell. *We therefore conclude that the quenching efficiencies reported here reflect the effect of the applied field on the fluorescent state of the PPVs rather than the effect of injected charges*. Moreover, in experimental configurations in which charge carriers are injected,[37,44,80] the polymer emission is seen to increase or decrease depending on whether holes or electrons are injected into the material. In contrast, quenching is seen for both the positive and negative phases of the applied AC field in the EF configuration.

Other important experimental parameters that determine the degree of quenching observed are the chain length and local density of PPV chains within the sample, with the latter being directly related to the probability of interchain contacts. Earlier studies using PPV-like polymers in which the conjugation was interrupted by using synthetic means[41,42] showed that those polymers with a longer effective conjugation length exhibited greater field-induced quenching efficiency. This result is in accord with the present study in which the chain-length dependence of the quenching probability is mapped out systematically. Likewise, several concentration studies have shown that exciton dissociation is favored by interchain contacts in PPV-type polymers,[33,36−38,40,42,81−83] though the question of whether dissociation could be seen on a single chain has been controversial.[55,56] The studies reported here were performed at concentrations that are over a factor of 100 lower than the lowest that have been studied by Deussen et al. in polymer matrixes.[38] To confirm the absence of concentration effects on our results, we examined OPPV-13 in a range of concentrations between $1 \times 10^{-5}$ M and $6 \times 10^{-8}$ M and found that the quenching efficiency varied relatively weakly over this range (from 0.3% ± 0.02% to 0.2% ± 0.1% with the larger error bars at low concentration being due to the poorer signal-to-noise of the spectra (data not shown)). Moreover, because our samples were entrained in a solvent glass, phase segregation effects that arise in polymer matrixes that can increase the local concentration of the dopant material are minimized.[84] *Our results show convincingly that a significant degree of quenching is single*

*chain in origin.* The fact that the quenching is ~50% greater in MEH-PPV than in OPPV-13 may reflect the additional favorable effects of interchain contacts possible only in the MEH-PPV. In comparison, Tolbert and co-workers[83,85] studied MEH-PPV contained in silicate pores of various sizes and observed a factor of 2 enhancement in the formation of polarons for MEH-PPV contained in pores large enough to accommodate more than one chain as compared to that in isolated chains confined to the smaller pores. Studies are currently underway in our group to specifically examine the effect of chain−chain contacts on the fluorescence quenching efficiency through the use of oligomer aggregates.

In summary, as it is well-known that factors such as casting conditions, solvent, and matrix can affect the effective conjugation length and the degree of chain−chain contacts in MEH-PPV,[66,86−91] variations in sample parameters may in part explain the range of quenching efficiencies reported in the literature. This also points to the importance of isolating these factors in deriving an understanding of the mechanism of exciton dissociation in PPV-like systems. The present study and others[83] are steps toward the realization of this goal.

The appropriate mechanisms to describe the fluorescence quenching experiments described here must allow for quenching to be observed in highly dilute samples having relatively short chains and not require the injection of charges into the matrix. Moreover, they must be consistent with the apparently linear scaling behavior of quench with inverse chain length that is observed, at least for the oligomers. In the following section, we consider mechanisms that could explain these observations.

### Quenching Mechanisms in Isolated Molecular Systems

Under our experimental conditions, the photophysical properties of the oligomers are those of isolated systems. We estimate the average distance between oligomers in glassy solvents to be on the order of 500 Å at the concentrations used in this experiment (~$10^{-6}$ M). At this distance, there is an exceedingly small probability of either energy transfer from neutral $S_1$ excitons to lower-energy nonemissive trap states located on neighboring oligomers or charge transfer between neighboring chains to form lower-energy weakly emissive excimers. *Therefore, the field-induced fluorescence quenching behavior we observe in oligomers reflects the interaction of relaxed* $S_1$ *excitons on isolated chains with the external electric field.*

In general, an external electric field can be used to overcome the exciton binding energy ($\boldsymbol{E}_b$) and dissociate the exciton if the energy gained by stabilization of the charge-separated species exceeds the energy cost of its formation. By using the measured $tr\Delta\tilde{\alpha}$ values for the oligomeric model compounds, we next estimate, as a function of chain length, the field strengths necessary to overcome the exciton binding energy.

A dipole placed in an electric field will reorient to minimize its potential energy.[92] The dipole potential energy is a function of dipole orientation relative to the external field, the external field magnitude, and the magnitude of the dipole that depends on the separation between the two charges. For a fixed isotropic sample of dipoles, a distribution of dipole potential energies within the field would be observed. In an analogous fashion, polarization of excitons in an applied field leads to the formation of dipoles. If we approximate an exciton in the relaxed $S_1$ state as a field-induced dipole, or geminate e−h pair, we can ascertain the stabilizing effects of the electric field on the geminate e−h pair. If the potential energy drop of the applied electric field across the dipole exceeds its Coulomb potential (or "binding" potential) exciton dissociation can occur. This condition for dissociation is described by the following inequality modified from its original form in ref 33 to model the effects of oligomer chain length on the exciton binding potential,[93]

$$(eFL_r \cos\theta) - \left(\frac{e^2}{4\pi\epsilon_0\epsilon_r L_r}\right) \geq 0 \qquad (6)$$

In eq 6, the first term on the left describes the angular dependence to the stabilization energy of the geminate e−h pair in an applied electric field, $F$, and the second term describes the exciton binding energy. $L_r$ is the exciton delocalization length and is interpreted as the extent of one-dimensional charge delocalization in the relaxed excited state. The dielectric constant of exciton environment is $\epsilon_r$. Here we approximate $\epsilon_r$ of MTHF by using the refractive index as $\eta^2 = \epsilon_r$ with $\eta = 1.4$.[94,95] because the environment is a low-temperature glass in which the solvent molecules cannot reorient to a significant degree to stabilize the dipole. Moreover, the use of the solvent refractive index is appropriate because our samples are at high dilution.[96] The symbol $\theta$ refers to the angle between the molecular transition moment (the polarization direction of the exciton) and the applied electric field vector determined by experimental parameters used in EF. The remaining terms are the charge on the electron ($e$) and the vacuum permittivity ($\epsilon_0$).

According to eq 6, the applied electric field dissociates the exciton and stabilizes the charge-separated state when the difference between the two terms is positive valued. In other words, when the dipole thus formed gains sufficient potential energy by interaction with the external field to overcome the attractive Coulombic force binding the electron and hole together. The result is the formation of a nonemissive charge-transfer state. By using the values of $tr\Delta$ measured via EF, we can derive $L_r$ for each oligomer and for MEH-PPV from simple geometric arguments.

Our formalism for extracting $L_r$ from $tr\Delta\tilde{\alpha}$ is as follows: In oligomers isolated in solvent glasses, the value of $tr\Delta\tilde{\alpha}$ is the sum of the exciton polarizability over three dimensions (i.e., $tr\Delta\tilde{\alpha} = \Delta\alpha_{xx} + \Delta\alpha_{yy} + \Delta\alpha_{zz}$). Because the value of $tr\Delta\tilde{\alpha}$ is dominated by the polarizability component in the direction of the long axis of the molecule (i.e., $tr\Delta \approx \Delta\alpha_{xx}$), the molecule can be modeled as an ellipse and the linear exciton delocalization length $L_r$ can be calculated from the formula for the volume of an ellipse (eq 7).

$$L_r = \frac{3}{4}\frac{tr\Delta\alpha}{(2.6\ \text{Å})^2\pi} \qquad (7)$$

There, 2.6 Å is the short molecular axis distance measured from a single PV unit.[97] $L_r$ values calculated from eq 7 are as follows (in order of increasing chain length): 5 ± 1 Å, 18 ± 2 Å, 35 ± 9 Å, 60 ± 18 Å, and 70 ± 7 Å (MEH-PPV). We find exciton delocalization lengths calculated from eq 7 are in good agreement with oligomer lengths calculated using AM1.[97]

Substituting these delocalization lengths back into eq 6, we calculated the critical field strengths necessary to dissociate the exciton into a charge-separated state in each of the oligomers. These values have been determined by assuming that the quench will be maximal for those oligomers oriented parallel to the applied field ($\theta \approx 0°$). They are, in order of increasing chain length (OPPV-3 to MEH-PPV): 30 ± 6, 2.0 ± 0.2, 0.5 ± 0.1, 0.2 ± 0.06, and 0.15 ± 0.02 MV/cm. This trend would predict that only chains longer than 9 units will exhibit measurable field-induced quenching at our field strengths. From a plot (Figure 8) of critical field strength versus inverse chain length, the field dependence of exciton dissociation is quadratic with inverse

conjugation length. Barford et al. found a similar result while studying the relationship between chain length and exciton binding energy by using density functional theory in polymers of varying conjugation length.[98] The correlation between chain length and the magnitude of fluorescence quench will be elaborated below.

Not surprisingly, a comparison of the critical electric fields calculated above to the applied field strength in EF (~0.3 MV/cm) demonstrates that the shorter oligomers are more difficult to destabilize in the relaxed $S_1$ state than the longer oligomers, OPPV-9 and OPPV-13. This conclusion is supported by the fact that no fluorescence quench is observed in the OPPV-3 oligomer despite its strong emission. In contrast, for the longer oligomers, the larger delocalization length of the exciton implies that the electron and hole are sufficiently well separated to allow on-chain charge separation and subsequent dissociation to occur in at least some fraction of the molecules.

One factor that can significantly affect the degree of quenching observed is the direction of the external electric field vector. For example, consider OPPV-13, for which the minimum field strength to dissociate an exciton is calculated to be $0.2 \pm 0.06$ MV/cm, assuming it is oriented parallel to the external field vector. Molecules oriented at some other angle to the field ($\theta$ in eq 6) will feel a weaker effective field. For each oligomer, the angle beyond which the field is too small to promote exciton dissociation can be calculated by rearranging and solving for $\vec{F}$ in eq 6 as a function of $\theta$. This yields tolerance angles of $\pm$ ~60° for OPPV-13, dramatically decreasing with chain length to less than 3° in OPPV-5. As a result, the quenching efficiency for the shorter oligomers is somewhat underestimated because relatively few chains will be optimally aligned with the field in a random sample.

It is of interest to compare the quenching efficiency seen in the oligomers to that observed in MEH-PPV itself. By examining Figure 8 more carefully, we find that, though the data is somewhat sparse, the quenching efficiency in MEH-PPV is at most ~60% greater than what would be predicted from a linear extrapolation to infinite chain length from the trend seen in the oligomers. Even without making any extrapolation, the quenching in MEH-PPV is about three times larger than in the longest oligomer studied (OPPV-13). There are several factors that could contribute to the somewhat higher efficiency of quenching in MEH-PPV relative to the isolated oligomer species. One that has been frequently invoked is the presence of interchain contacts in the isolated folded polymer, which allows the electron and hole to separate onto different chains, facilitating dissociation. The second is a change in the local dielectric environment caused by neighboring chains in the polymer. As shown by Moore et al.,[99,100] neighboring chains can solvate the nascent electron−hole pair more efficiently than can the solvent glass because of their higher effective index of refraction. As can be seen from eq 6, a higher index of refraction, and therefore a higher local dielectric constant, can decrease the exciton binding energy. However, calculating the effective field strength based on a refractive index measured from MEH-PPV thin films (~1.6) revealed a negligible difference between field strengths calculated using the solvent refractive index and that of the thin films. Finally, because the polymer consists of a distribution of conjugation lengths, segments longer than our longest oligomer (OPPV-13) may be present to which rapid energy migration would be expected to occur. The consequence may be enhanced field-induced quenching because, as described earlier, the probability of exciton dissociation on single chains is higher for chains with longer effective conjugation lengths.

Of the three effects discussed, the latter would be the least likely to explain the results. This is the case because, as noted earlier, the saturation length for exciton delocalization, as measured by the shift in the absorption band with chain length or by the increase of $tr\Delta\tilde{\alpha}$, is roughly 8−13 units. In addition, preliminary evidence of reduced fluorescence quench in oligomer chain lengths longer than 13-monomer units has been found. By using a 17-monomer unit oligomer (OPPV-17), we have found fluorescence quench decreases by roughly 40% relative to the quench observed in OPPV-13 at comparable field strengths. This suggests that the exciton dissociation probability does *not* continue to increase with increasing oligomer length beyond a saturation length of 13 units. Further testing of this hypothesis is underway, and the results will appear in a future communication from this group.

By turning to the role of interchain interactions in promoting field-induced quenching, elegant experiments by Tolbert et al.[83] have demonstrated an increased efficiency of polaron formation when two MEH-PPV chains are allowed to interact with one another relative to that in a single extended chain. To clarify the effects of stacking interactions in our measurements with oligomeric systems, we are in the process of examining field-induced fluorescence quenching in *aggregates* of oligomers in which interchain interactions are presumably promoted. Though, in many cases, aggregation of PPV-like molecules decreases their fluorescence intensity, the emission is still sufficient to observe field-induced quenching. This will be discussed in a future communication. Comparing the field-induced quenching of MEH-PPV in solvents that favor an extended conformation to that in solvents that favor folding may also prove useful in addressing this issue.

Finally, as noted earlier, it is ultimately essential to definitively assign the mechanism responsible for the observed emission quenching to polaron formation versus other known phenomena in organic systems such as a field-induced change in internal conversion and so forth.[45,46,101] The "back-of-the-envelope" calculations presented above suggest that exciton dissociation is indeed possible under our experimental conditions, at least for the longer-chain oligomers. Nonetheless, efforts are in progress to find direct evidence for or against field-induced formation of polarons in highly dilute MEH-PPV and oligomer-doped solvent glass and polymer matrixes via photoinduced absorption.[83,85] This, when coupled with work in progress to perform a systematic investigation of the variation in field-induced quenching with energy gap (which can be varied by chemical substitution), will enable a more complete picture of the mechanism of field-induced quenching in PPV systems to emerge.

## Conclusions

The optical and electronic properties of MEH-PPV and a series of oligomeric model compounds have been studied using electroabsorption and electrofluorescence spectroscopy. On the basis of the similarity between electronic properties measured by both techniques, geometrical changes associated with vibrational cooling and planarization of the Franck−Condon excited state do not significantly alter the electronic properties of $S_1$ excitons prior to emission. An electric-field-induced fluorescence quench was observed in both dilute oligomer solutions and the polymer, with the magnitude of quench being proportional to the molecular chain length in the oligomer species. The possibility that field-induced exciton dissociation is the cause of the observed quenching was examined and model calculations were performed to demonstrate the feasibility of this mechanism for oligomers in dilute solvent glasses.

**Acknowledgment.** L.A.P. acknowledges NSF CHE-0109761 and the Center for Molecular Analysis at CMU for use of the absorption spectrometer, and we thank Dr. Sebastian Wachsmann-Hogiu for setting up the electrofluorescence spectrometer and Drs. Nobuhiro Ohta, Keith Walters, and Benjamin Schwartz for helpful discussions.

## References and Notes

(1) Burroughes, J. H.; Bradley, D. D. C.; Brown, A. R.; Marks, R. N.; Mackay, K.; Friend, R. H.; Burns, P. L.; Holmes, A. B. *Nature (London)* **1990**, *347*, 539−541.

(2) Mitschke, U.; Bauerle, P. *J. Mater. Chem.* **2000**, *10*, 1471−1507.

(3) Yang, Y.; Heeger, A. J. *Polym. Mater. Sci. Eng.* **1995**, *72*, 454.

(4) Shaked, S.; Tal, S.; Roichman, Y.; Razin, A.; Xiao, S.; Eichen, Y.; Tessler, N. *Adv. Mater. (Weinheim, Ger.)* **2003**, *15*, 913−916.

(5) Muratsubaki, M.; Furukawa, Y.; Noguchi, T.; Ohnishi, T.; Fujiwara, E.; Tada, H. *Chem. Lett.* **2004**, *33*, 1480−1481.

(6) Sakanoue, T.; Fujiwara, E.; Yamada, R.; Tada, H. *Chem. Lett.* **2005**, *34*, 494−495.

(7) Braun, D.; Heeger, A. J. *Appl. Phys. Lett.* **1991**, *58*, 1982−1984.

(8) Yoshino, K.; Tada, K.; Fujii, A.; Conwell, E. M.; Zakhidov, A. A. *IEEE Trans. Electron Devices* **1997**, *44*, 1315−1324.

(9) Gao, J.; Hide, F.; Wang, H. *Synth. Met.* **1997**, *84*, 979−980.

(10) Coakley, K. M.; McGehee, M. D. *Chem. Mater.* **2004**, *16*, 4533−4542.

(11) Roitman, D. B.; Sheats, J. R. In *U. S.*; Agilent Technologies, Inc.: Palo Alto, CA, 2000; p 6.

(12) Diaz-Garcia, M. A.; Hide, F.; Schwartz, B. J.; Andersson, M. R.; Pei, Q.; Heeger, A. J. *Synth. Met.* **1997**, *84*, 455−462.

(13) Hide, F., 1997.

(14) McGehee, M. D.; Diaz-Garcia, M. A.; Hide, F.; Gupta, R.; Miller, E. K.; Moses, D.; Heeger, A. J. *Appl. Phys. Lett.* **1998**, *72*, 1536−1538.

(15) Friend, R. H.; Bradley, D. D. C.; Townsend, P. D. *J. Phys. D: Appl. Phys.* **1987**, *20*, 1367−1384.

(16) Horvath, A.; Baessler, H.; Weiser, G. *Phys. Status Solidi B* **1992**, *173*, 755−764.

(17) Horvath, A.; Weiser, G. *Mol. Cryst. Liq. Cryst. Sci. Technol., Sect. A* **1994**, *256*, 79−86.

(18) Liess, M.; Jeglinski, S.; Vardeny, Z. V.; Ozaki, M.; Yoshino, K.; Ding, Y.; Barton, T. *Phys. Rev. B: Condens. Matter* **1997**, *56*, 15712−15724.

(19) Liess, M.; Lane, P. A.; Kafafi, Z. H.; Hamaguchi, M.; Yzaki, M.; Yoshino, K.; Vardeny, Z. V. *Proc. SPIE−Int. Soc. Opt. Eng.* **1997**, *3142*, 150−160.

(20) Martin, S. J.; Mellor, H.; Bradley, D. D. C.; Burn, P. L. *Opt. Mater. (Amsterdam)* **1998**, *9*, 88−93.

(21) Wachsmann-Hogiu, S.; Peteanu, L. A.; Liu, L. A.; Yaron, D. J.; Wildeman, J. *J. Phys. Chem. B* **2003**, *107*, 5133−5143.

(22) Sariciftci, N. S. *Primary Photoexcitations in Conjugated Polymers: Molecular Exciton Versus Semiconductor Band Model*, 1st ed.; World Scientific Publishing Company; River Edge, NJ, 1997.

(23) Osterbacka, R.; Wohlgenannt, M.; Shkunov, M.; Chinn, D.; Vardeny, Z. V. *J. Chem. Phys.* **2003**, *118*, 8905−8916.

(24) Liptay, W. In *Excited States*; Lim, E. C., Ed.; Academic Press: New York, 1974; Vol. 1, pp 129−229.

(25) Baumann, W.; Bischof, H. *J. Mol. Struct.* **1985**, *129*, 125−136.

(26) Warman, J. M.; Gelinck, G. H.; Piet, J. J.; Suykerbuyk, J. W. A.; De Haas, M. P.; Langeveld-Voss, B. M. W.; Janssen, R. A. J.; Hwang, D.-H.; Holmes, A. B.; Remmers, M.; Neher, D.; Mullen, K.; Bauerle, P. *Proc. SPIE−Int. Soc. Opt. Eng.* **1997**, *3145*, 142−149.

(27) Gelinck, G. H.; Piet, J. J.; Wegewijs, B. R.; Mullen, K.; Wildeman, J.; Hadziioannou, G.; Warman, J. M. *Phys. Rev. B: Condens. Matter* **2000**, *62*, 1489−1491.

(28) van der Horst, J. W.; Bobbert, P. A.; de Jong, P. H. L.; Michels, M. A. J.; Siebbeles, L. D. A.; Warman, J. M.; Gelinck, G. H.; Brocks, G. *Chem. Phys. Lett.* **2001**, *334*, 303−308.

(29) Antoniadis, H.; Hsieh, B. R.; Abkowitz, M. A.; Jenekhe, S. A.; Stolka, M. *Synth. Met.* **1994**, *62*, 265−271.

(30) Cornil, J.; Dos Santosa, D. A.; Silbey, R.; Bredas, J. L. *Synth. Met.* **1999**, *101*, 492−495.

(31) Halls, J. J. M.; Cornil, J.; Dos Santos, D. A.; Hwang, D. H.; Holmes, A. B.; Bredas, J. L.; Friend, R. H. *Synth. Met.* **1999**, *101*, 105−106.

(32) Bredas, J.-L.; Beljonne, D.; Coropceanu, V.; Cornil, J. *Chem. Rev.* **2004**, *104*, 4971−5003.

(33) Arkhipov, V. I.; Baessler, H.; Deussen, M.; Goebel, E. O. *Phys. Rev. B: Condens. Matter* **1995**, *52*, 4932−4940.

(34) Arkhipov, V. I.; Baessler, H.; Deussen, M.; Goebel, E. O.; Lemmer, U.; Mahrt, R. F. *J. Non-Cryst. Solids* **1996**, *198−200*, 661−664.

(35) Arkhipov, V. I.; Baessler, H. *Phys. Status Solidi A* **2004**, *201*, 1152−1187.

(36) Kersting, R.; Lemmer, U.; Deussen, M.; Bakker, H. J.; Mahrt, R. F.; Kurz, H.; Arkhipov, V. I.; Baessler, H.; Goebel, E. O. *Phys. Rev. Lett.* **1994**, *73*, 1436−1439.

(37) Deussen, M.; Scheidler, M.; Baessler, H. *Synth. Met.* **1995**, *73*, 123−129.

(38) Deussen, M.; Haring Bolivar, P.; Wegmann, G.; Kurz, H.; Baessler, H. *Chem. Phys.* **1996**, *207*, 147−157.

(39) Esteghamatian, M.; Popovic, Z. D.; Xu, G. *J. Phys. Chem.* **1996**, *100*, 13716−13719.

(40) Khan, M. I.; Bazan, G. C.; Popovic, Z. D. *Chem. Phys. Lett.* **1998**, *298*, 309−314.

(41) Khan, M. I.; Renak, M. L.; Bazan, G. C.; Popovic, Z. *J. Am. Chem. Soc.* **1997**, *119*, 5344−5347.

(42) Pfeffer, N.; Neher, D.; Remmers, M.; Poga, C.; Hopmeier, M.; Mahrt, R. *Chem. Phys.* **1998**, *227*, 167−178.

(43) Schweitzer, B.; Arkhipov, V. I.; Bassler, H. *Chem. Phys. Lett.* **1999**, *304*, 365−370.

(44) McNeill, J. D.; O'Connor, D. B.; Adams, D. M.; Barbara, P. F. *J. Phys. Chem. B* **2001**, *105*, 76−82.

(45) Wahadoszamen, M.; Nakabayashi, T.; Ohta, N. *Chem. Phys. Lett.* **2004**, *387*, 124−129.

(46) Nakabayashi, T.; Wahadoszamen, M.; Ohta, N. *J. Am. Chem. Soc.* **2005**, *127*, 7041−7052.

(47) Walters, K. A.; Gaal, D. A.; Hupp, J. T. *J. Phys. Chem. B* **2002**, *106*, 5139−5142.

(48) Boxer, S. G. *Photosynth. React. Cent.* **1993**, *2*, 179−120.

(49) Lockhart, D. J.; Boxer, S. G. *Proc. Natl. Acad. Sci. U.S.A.* **1988**, *85*, 107−111.

(50) Yu, J.; Hayashi, M.; Lin, S. H.; Liang, K. K.; Hsu, J. H.; Fann, W. S.; Chao, C.-I.; Chuang, K.-R.; Chen, S.-A. *Synth. Met.* **1996**, *82*, 159−166.

(51) Lim, S.-H.; Bjorklund, T. G.; Bardeen, C. J. *Chem. Phys. Lett.* **2001**, *342*, 555−562.

(52) Bredas, J.-L.; Cornil, J.; Beljonne, D.; Dos Santos, D. A.; Shuai, Z. *Acc. Chem. Res.* **1999**, *32*, 267−276.

(53) Lagowski, J. B. *THEOCHEM* **2002**, *589−590*, 125−137.

(54) Siebbeles, L. D. A.; Grozema, F. C.; De Haas, M. P.; Warman, J. M. *Radiat. Phys. Chem.* **2004**, *72*, 85−91.

(55) Vissenberg, M. C. J. M.; de Jong, M. J. M. *Phys. Rev. Lett.* **1996**, *77*, 4820−4823.

(56) Conwell, E. M. *Phys. Rev. Lett.* **1997**, *78*, 4301.

(57) Gill, R. E.; Hilberer, A.; van Hutten, P. F.; Berentschot, G.; Werts, M. P. L.; Meetsma, A.; Wittmann, J.-C.; Hadziioannou, G. *Synth. Met.* **1997**, *84*, 637−638.

(58) Neef, C. J.; Ferraris, J. P. *Macromolecules* **2000**, *33*, 2311−2314.

(59) Bublitz, G. U.; Boxer, S. G. *Annu. Rev. Phys. Chem.* **1997**, *48*, 213−242.

(60) Leng, J. M.; Jeglinski, S.; Wei, X.; Benner, R. E.; Vardeny, Z. V.; Guo, F.; Mazumdar, S. *Phys. Rev. Lett.* **1994**, *72*, 156−159.

(61) Hagler, T. W.; Pakbaz, K.; Heeger, A. J. *Phys. Rev. B: Condens. Matter* **1995**, *51*, 14199−14206.

(62) Martin, S. J.; Bradley, D. D. C.; Lane, P. A.; Mellor, H.; Burn, P. L. *Phys. Rev. B: Condens. Matter* **1999**, *59*, 15133−15142.

(63) Woo, H. S.; Lhost, O.; Graham, S. C.; Bradley, D. D. C.; Friend, R. H.; Quattrocchi, C.; Bredas, J. L.; Schenk, R.; Muellen, K. *Synth. Met.* **1993**, *59*, 13−28.

(64) Harrison, N. T.; Baigent, D. R.; Samuel, I. D. W.; Friend, R. H.; Grimsdale, A. C.; Moratti, S. C.; Holmes, A. B. *Phys. Rev. B: Condens. Matter* **1996**, *53*, 15815−15822.

(65) Yu, J.; Hu, D.; Barbara, P. F. *Science (Washington, D.C.)* **2000**, *289*, 1327−1330.

(66) Huser, T.; Yan, M. *J. Photochem. Photobiol., A* **2001**, *144*, 43−51.

(67) Schwartz, B. J.; Nguyen, T.-Q.; Wu, J.; Tolbert, S. H. *Synth. Met.* **2001**, *116*, 35−40.

(68) Grage, M. M. L.; Wood, P. W.; Ruseckas, A.; Pullerits, T.; Mitchell, W.; Burn, P. L.; Samuel, I. D. W.; Sundstrom, V. *J. Chem. Phys.* **2003**, *118*, 7644−7650.

(69) Jeglinski, S. A.; Vardeny, Z. V.; Ding, Y.; Barton, T. *Mol. Cryst. Liq. Cryst. Sci. Technol., Sect. A* **1994**, *256*, 87−96.

(70) Lane, P. A.; Liess, M.; Vardeny, Z. V.; Hamaguchi, M.; Ozaki, M.; Yoshino, K. *Synth. Met.* **1997**, *84*, 641−642.

(71) Liess, M.; Jeglinski, S.; Lane, P. A.; Vardeny, Z. V. *Synth. Met.* **1997**, *84*, 891−892.

(72) Fluorescence excitation anisotropy experiments were performed on various oligomers. Energy transfer between oligomers as a result of aggregation would lead to increased steady-state fluorescence depolarization. Steady-state anisotropy values of 0.25 ± 0.05 were measured for the OPPVs as would be expected from isolated chromophores.

(73) Arkhipov, V. I.; Baessler, H.; Emelianova, E. V.; Gerhard, A.; Gulbinas, V.; Hayer, A. *Mol. Cryst. Liq. Cryst. Sci. Technol., Sect. B* **2002**, *29*, 175−182.

(74) Arkhipov, V. I.; Emelianova, E. V.; Tak, Y. H.; Bassler, H. *J. Appl. Phys.* **1998**, *84*, 848−856.

(75) Sheats, J. R.; Chang, Y.-L.; Roitman, D. B.; Stocking, A. *Acc. Chem. Res.* **1999**, *32*, 193−200.

(76) Scheblykin, I.; Zoriniants, G.; Hofkens, J.; De Feyter, S.; Van der Auweraer, M.; De Schryver, F. C. *ChemPhysChem* **2003**, *4*, 260−267.

(77) Arkhipov, V. I.; Emelianova, E. V.; Bassler, H. *Phys. Rev. B: Condens. Matter* **2004**, *70*, 205205/205201−205205/205207.

(78) Gesquiere, A. J.; Park, S.-J.; Barbara, P. F. *Eur. Polym. J.* **2004**, *40*, 1013−1018.

(79) Park, S.-J.; Gesquiere, A. J.; Yu, J.; Barbara, P. F. *J. Am. Chem. Soc.* **2004**, *126*, 4116−4117.

(80) Adams, D. M.; Kerimo, J.; Liu, C.-Y.; Bard, A. J.; Barbara, P. F. *J. Phys. Chem. B* **2000**, *104*, 6728−6736.

(81) Moses, D.; Wang, J.; Heeger, A. J.; Kirova, N.; Brazovski, S. *Synth. Met.* **2001**, *119*, 503−506.

(82) Arkhipov, V. I.; Bassler, H. *Handb. Lumin. Disp. Mater. Devices* **2003**, *1*, 279−342.

(83) Cadby, A.; Tolbert, S. H. *Polym. Prepr. (Am. Chem. Soc., Div. Polym. Chem.)* **2004**, *45*, 208−209.

(84) Chou, H.-L.; Hsu, S.-Y.; Wei, P.-K. *Polymer* **2005**, *46*, 4967−4970.

(85) Cadby, A.; Tolbert, S. H. *J. Phys. Chem. B* **2005**, *109*, 17879−17886.

(86) Nguyen, T.-Q.; Doan, V.; Schwartz, B. J. *J. Chem. Phys.* **1999**, *110*, 4068−4078.

(87) Huser, T.; Yan, M.; Rothberg, L. J. *Proc. Natl. Acad. Sci. U.S.A.* **2000**, *97*, 11187−11191.

(88) Nguyen, T.-Q.; Kwong, R. C.; Thompson, M. E.; Schwartz, B. J. *Synth. Met.* **2001**, *119*, 523−524.

(89) Schaller, R. D.; Snee, P. T.; Johnson, J. C.; Lee, L. F.; Wilson, K. R.; Haber, L. H.; Saykally, R. J.; Nguyen, T.-Q.; Schwartz, B. J. *J. Chem. Phys.* **2002**, *117*, 6688−6698.

(90) Rothberg, L. *Proc. Int. Sch. Phys "Enrico Fermi"* **2002**, *149th*, 299−316.

(91) Hsu, J.-H.; Hayashi, M.; Lin, S.-H.; Fann, W.; Rothberg, L. J.; Perng, G.-Y.; Chen, S.-A. *J. Phys. Chem. B* **2002**, *106*, 8582−8586.

(92) Tipler, P. A. *Physics for Scientists and Engineers*, 4th ed.; W. H. Freeman and Company: New York, 1999.

(93) Eq 16 in ref 33 establishes the exciton binding energy ($E_b$) as an energy criterion to exciton dissociation. According to the authors, an optical excitation (exciton) can dissociate if the gain of electrostatic energy is sufficient to (1) stabilize separation of charge carriers, and (2) prevent their recombination within the Coulomb potential well. In eq 6 of the current report, we consider exciton dissociation to be a 1D Onsager-like process where dissociation occurs on-chain in the oligomers if the energy difference between the exciton in a strong external field (first term) exceeds its Coulombic binding energy (second term).

(94) Weast, R. C., Ed. *CRC Handbook of Chemistry and Physics*, 1st ed.; CRC Press: Boca Raton, 1988.

(95) Fowles, G. R. *Introduction to Modern Optics*, 2nd ed.; Dover Publications: New York, 1975.

(96) In MTHF, low-temperature dielectric measurements by Richert et al. [*Chem. Phys. Lett.* **1993**, *216*, 223] taken below the solvent glass transition temperature have shown the dielectric constant increases from ∼1.4 at 298 K to ∼19 at 77 K. Maxwell's dispersion relationship, used in eq 6 to estimate the dielectric constant of MTHF, becomes less valid as the solvent temperature decreases. The effect of increasing the dielectric constant in eq 6 would be to reduce the exciton binding potential by an order of magnitude, making exciton dissociation more probable in the presence of an applied field.

(97) Delocalization length (∼5.2 Å) of 1 PV unit was calculated in CS Chem3D Ultra version 6.0 using CS MOPAC Pro with the AM1 Hamiltonian. The structure was highly planar (RMS deviation ∼0.005 Å). Distances were measured between the *para*-carbon opposite the vinyl group and the outermost vinyl carbon. The best estimate for the short molecular axis of 1 PV for this geometry is 2.6 Å.

(98) Barford, W.; Bursill, R. J. *Synth. Met.* **1997**, *89*, 155−157.

(99) Moore, E. E.; Yaron, D. *Synth. Met.* **1997**, *85*, 1023−1024.

(100) Barford, W.; Bursill, R. J.; Yaron, D. *Phys. Rev. B: Condens. Matter* **2004**, *69*, 155203/155201−155203/155205.

(101) Iwaki, Y.; Ohta, N. *Chem. Lett.* **2000**, 894−895.